Multigap-Waveguide Liquid Crystal Phase Shifter at Ka-Band

Marc Späth, *Graduate Student Member, IEEE*, Robin Neuder, Martin Schüßler, Rolf Jakoby, and Alejandro Jiménez-Sáez, *Member, IEEE*

***Abstract*— This letter presents for the first time an innovative waveguide structure, the multigap-waveguide (MGWG), utilizing liquid crystal (LC) technology to develop a continuously tunable phase shifter at Ka-band. In contrast to existing LC phase shifters, this design eliminates the need for polymer films or thin-film stepped impedance structures to control LC molecules. The inclusion of a gap waveguide flange ensures an individual electrical biasing of the four electrodes. The proposed design achieves a maximum differential phase of 281° in the frequency range from 24 to 38.5 GHz, with insertion losses ranging from 2.1 to 3.1 dB. The maximum figure of merit (FoM) is 105°/dB.**

***Index Terms*— K-band, liquid crystals (LCs), millimeter wave devices, phase shifters, tunable circuits and devices.**

I. Introduction

GLOBAL mobile subscriptions have exceeded the planetary human population [1], driving the need for increased data rates into higher bands, such as the Ka-band. The upcoming 5G/6G communication network aims to provide the envisioned data rates by counteracting the occurring higher path losses with high-gain antennas. To establish a communication link between satellites, or a base station and a user, the beam needs to be reconfigurable. Hence, steerable phased antenna arrays could be a solution.

Based on the configuration of the beamforming network, distinctions can be made among digital, analog, and hybrid beamforming implementations [2]. Digital beamforming enables maximum system capacity, but requires a complete RF chain and a data converter per antenna element, resulting in high power consumption [3]. Hybrid beamforming, integrating RF components and digital control, offers a balanced solution for mm-wave communication with reduced power consumption compared to digital beamforming. Consequently, the utilization of analog phase shifters is commonly chosen in mm-wave communication [4]. These are implemented via micro-electro-mechanical systems (MEMSs) [5], semiconductors [6], or liquid crystals (LCs). MEMS-based phase shifters, as well as semiconductor (CMOS, varactor diode) ones, have the drawback of usually high losses, limited power handling capability, phase error, and sometimes they allow only discrete phase shifting. However, both technologies enable fast tuning.

In this letter, LC technology is employed for its capability to realize continuous tunability with low losses in the millimeter wave to terahertz range [7], though accompanied by a relatively moderate response time. However, LC components achieve high linearity and low power consumption during the tuning process. Various waveguide topologies have been employed in the development of tunable LC phase shifters. Notably, rectangular metallic waveguide LC phase shifters have demonstrated great performance, as reported in [8] and [9]. However, these devices necessitate integrated electrodes, which interact with the electromagnetic wave, resulting in increased losses. Moreover, the design of these electrodes require implementation as stepped impedance low-pass filters. An alternative tuning mechanism for LC molecules involves a rubbed polymer film applied to the transmission line surface [10]. This technology is limited to thin LC layer heights below, 200 μm and is therefore commonly employed in planar structures [10]. Yet, this biasing method has not achieved comparable performance to hollow waveguide technologies with integrated stepped impedance electrodes.

To address the aforementioned challenge, this work introduces an LC phase shifter based on a novel waveguide structure. Notably, this innovative configuration of four separated segments can be directly biased and eliminates the necessity for the incorporation of polymer films or stepped impedance structures. Instead of these conventional methods, the metallic walls of the waveguide itself are utilized for full electrical biasing by dividing the waveguide into four distinct segments. The technology of groove gap waveguide (GGW) is employed for each segment to ensure minimal leakage.

II. Tunable Multigap Waveguide LC Phase Shifter

A. Multigap-Waveguide

The GGW offers the unique advantage of dc-decoupled metal line sections at the top and bottom [11]. DC decoupling is achieved by the small gap between the bed of nails structure at the bottom and the top metal plate, in which no propagation is possible, due to an electromagnetic stopband. This GGW technology has been already used and proven for tunable LC phase shifters [12], where a voltage between the top and bottom metal is applied to tune the LC molecules. This principle led to the idea to occupy this concept to invent a novel waveguide structure out of four galvanic isolated GGW segments

Received 15 October 2024; revised 22 December 2024; accepted 6 January 2025. This work was supported by the Deutsche Forschungsgemeinschaft (DFG, German Research Foundation) under Project JA 921/80-1. *(Corresponding author: Marc Späth.)*

The authors are with the Institute of Microwave Engineering and Photonics (IMP), Technische Universität Darmstadt, 64289 Darmstadt, Germany (e-mail: marc.spaeth@tu-darmstadt.de).

Digital Object Identifier 10.1109/LMWT.2025.3527029

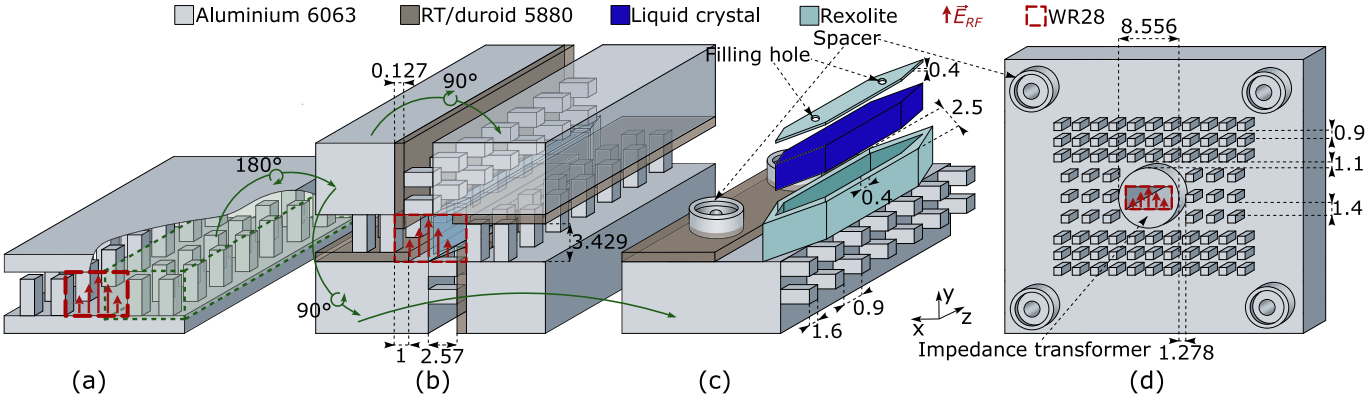

Fig. 1. (a) Evolution from a GGW toward the entire MGWG LC phase shifter is shown and (b) lower gap waveguide segment, featuring a tapered LC Rexolite container with inserted LC in an exploded view (c) is presented. (d) Gap waveguide flange with the WR28 waveguide in the center surrounded by a $\lambda/4$ transformer.

called multigap-waveguide (MGWG), shown in Fig. 1(b). The spacing between the pins and the opposite metal surface needs to be kept below $d < \lambda/4$, as then the bed of nail structure acts as a perfect magnetic conductor (PMC) and the opposite metallic surface acts as a perfect electrical conductor (PEC). Thus, wave propagation along the gaps between each GGW segment is prohibited. The GGW segments are arranged in a way, so that a WR28 (7.112×3.556 mm) waveguide is formed, which supports the TE_{10} fundamental mode and is highlighted with red dashed lines as shown in Fig. 1. The spacing d is achieved, by inserting a Rogers RT/duroid 5880 [13] substrate with $\varepsilon_r = 2.2$ and $\tan\delta = 9 \cdot 10^{-4}$ at 10 GHz with a thickness of 0.127 mm. This substrate serves not only as accurate spacing but also as electrical breakdown protection between the galvanic isolated segments.

B. LC Phase Shifter

To realize a phase shifter in the MGWG topology, the electrical length of the WR28 channel needs to be altered. This is achieved, by filling nematic LC, an anisotropic material, in a Rexolite container and positioning the container into the MGWG, as shown in Fig. 1(c). The Rexolite container is tapered to achieve better matching. The Rexolite possesses dielectric properties as $\varepsilon_r = 2.53$ and $\tan\delta = 6.6 \cdot 10^{-4}$. The orientation of the LC molecules can be altered by a low-frequency alternating electric field, specifically a 10 kHz square wave signal. If the molecule's long axis is oriented parallel to the electrical RF vector $\vec{E}_{\mathrm{RF}}$, as shown in Fig. 2(a), the effective permittivity and loss tangent for the employed GT7-29001 [14] mixture at 19 GHz is $\varepsilon_{r,||} = 3.53$ and $\tan\delta_{||} = 6.4 \cdot 10^{-3}$. If the molecules are oriented orthogonal to the $\vec{E}_{\mathrm{RF}}$, as shown in Fig. 2(b), the effective permittivity and loss tangent are changed to be $\varepsilon_{r,\perp} = 2.45$ and $\tan\delta_{r,\perp} = 1.16 \cdot 10^{-2}$. By adjusting the voltage between the two edge cases, all orientations and thus all permittivities in between can be achieved.

C. Gap Waveguide Flange

To conduct measurements via a WR28 coaxial to hollow waveguide flange, a fundamental issue emerges. Directly connecting the metallic flange to the MGWG is unfeasible, as it would create a short across all GGW segments. Thus, the concepts of a GGW is again employed to ensure galvanic isolation of all MGWG segments. The contactless GGW flange from [15] is taken as a reference and is further optimized, as in this case, the flange is not facing a planar metal plane, rather a more complex surface. Without optimization, the direct combination would lead to undesired resonances. The round metal elevation around the WR28 waveguide, presented in Fig. 1(d), acts as a $\lambda/4$ transformer and transforms the open into a short.

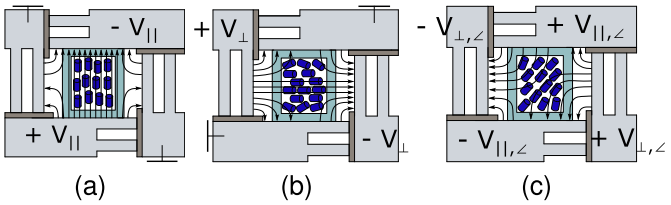

Fig. 2. Electrical biasing configurations to achieve. (a) Parallel, (b) orthogonal, and (c) intermediate orientation of the LC molecules is presented. The applied voltages to achieve the molecule orientations are: $V_{||} = 100$ V, $V_{\perp} = 245$ V, $V_{||,\angle} = 15$ V and $V_{\perp,\angle} = 200$ V. Different intermediate states can be achieved by varying the $\angle$ voltages.

III. Measurement Results

To perform measurements, the MGWG phase shifter and the gap waveguide flanges are mounted together with nylon screws, to ensure galvanic isolation. Further, in between the flange and the MGWG component, the same Rogers substrate as before is placed, to ensure shielding and to guarantee the specific spacing. Circular ring nylon spacers are strategically positioned on the metallic spacers depicted in Fig. 1(c) and (d) to provide additional assurance of proper spacing. The Rexolite component is milled in two halves and the cover is glued on top of the container with Norland Optical Adhesive 88 with $\varepsilon_r = 2.3$ and $\tan\delta = 0.022$ [16]. The Rexolite container is then positioned in the MGWG waveguide using small alignment slots. After the assembling, cables are soldered to the MGWG segments to steer the LC molecules, as shown in Fig. 3. A TRL calibration is performed on the plane of the WR28 coaxial to waveguide flanges, which are then screwed to the gap waveguide flanges. In Fig. 4, the simulated and measured S-parameters are presented. The case $\varepsilon_r = 2.7$ highlights that

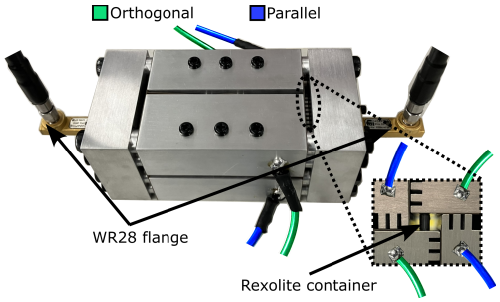

Fig. 3. Assembled MGWG phase shifter incorporates the gap waveguide flange connected to WR28 flanges, secured with Nylon screws. Green cables facilitate orthogonal biasing through soldering onto the metal, while blue cables serve for parallel orientation of the LC molecules.

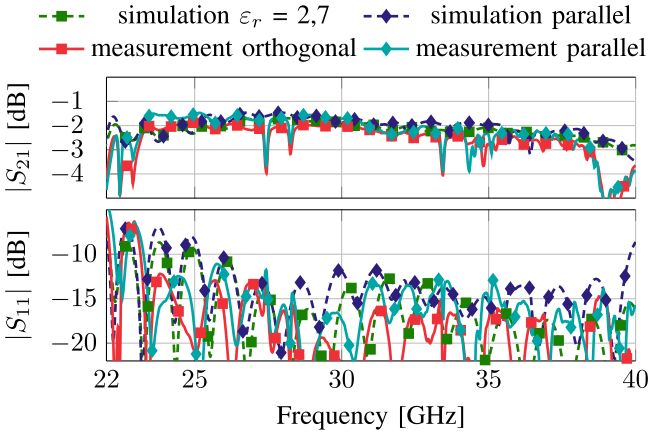

Fig. 4. Measured and simulated S-parameters for the orthogonal and parallel orientation of the LC. The tolerances and deviations appearing in the measured model are taken into account, same as the fact, that the orthogonal state is not fully achievable in the measurement.

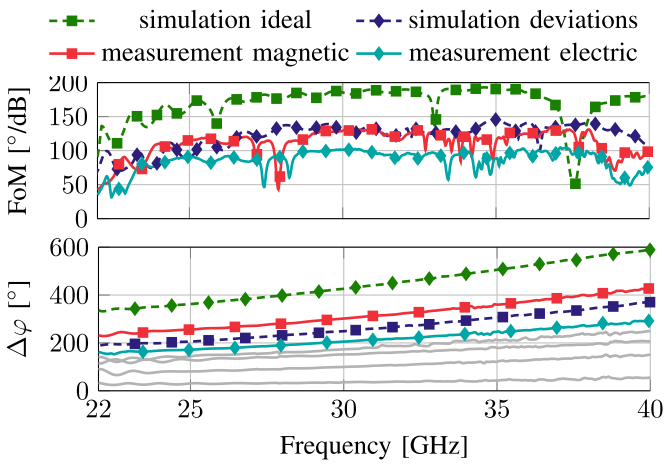

Fig. 5. Measured and simulated differential phase shift and FoM of the MGWG LC phase shifter. The ideal simulation does not account for tolerances and deviations from the manufactured design, while the deviations simulation includes effects such as air bubbles, glue, and rounded edges. The gray curves represent the differential phase shift for different voltage settings.

TABLE I

COMPARISON OF STATE-OF-THE-ART Ka-BAND PHASE SHIFTERS. THE MAXIMUM VALUES OF THE DIFFERENTIAL PHASE SHIFT, $\Delta\varphi$, AND THE FoM ARE GIVEN AT f_{OPT}

Topology	Technology	f [GHz]	$\Delta\varphi$ [°]	FoM [°/dB]	Ref.
Microstrip	CMOS	21 - 25	336	21	[6]
CPW	BST MIM	0 - 60	70	43	[18]
SIW	Varactor diode	18 - 22	200	50	[19]
RGW	LC	20 - 30	387	70	[12]
DGS-IMSL	LC	5 - 35	360	79	[10]
MGWG	LC	24 - 38.5	266	105	This work
Waveguide	LC	28 - 38	110	155	[9]

the orthogonal state cannot be fully reached due to fringing fields, which prevent complete alignment of molecules in the corners, as shown in Fig 2(b). The measured insertion loss (IL) in the frequency range from 24 to 38.5 GHz is 2.1 to 3.1 dB and the reflection is below −13 dB.

The measured and simulated differential phase shift $\Delta\varphi$ and figure-of-merit (FoM), defined as the ratio of $\Delta\varphi$ to the maximum IL $\mathrm{IL_{max}}$, are presented in Fig. 5. The simulation also includes deviations to account for manufacturing tolerances, such as air bubbles, glue, and rounded edges. Magnetic measurements were conducted by placing magnets either above and below the structure for parallel orientation or on the sides for orthogonal orientation. Magnetic biasing achieves the full tuning potential of the LC, resulting in a higher FoM compared to electrical biasing. At 30 GHz, the differential phase shift is 205 °, while the FoM reaches 100 °/dB between 28.5 and 31 GHz, peaking at 105 °/dB at 37.1 GHz. The response times [17] are measured as $\tau_{\mathrm{on}} < 1$ s and $\tau_{\mathrm{off}} = 684$ s. The total power consumption is in the range of 1.7e–12 W. Those losses accumulated due to capacitive equivalent series resistances between the elements. A comparison with state-of-the-art phase shifters, summarized in Table I, highlights the diverse trade-offs in design and performance. This work demonstrates a competitive FoM within the given frequency range, highlighting its potential among existing phase shifter technologies.

FoM improvements can be achieved by enhancing tunability and reducing insertion losses. The large electrode spacing creates an inhomogeneous electric field, limiting full orthogonal LC orientation. Additionally, air bubbles introduced during Rexolite container sealing cause permittivity changes, further restricting LC tuning potential. Solutions include optimizing the waveguide's width/height ratio, redesigning the Rexolite container, and minimizing glue usage to reduce insertion losses. Furthermore, wave propagation and resonances in the substrate between the flange and the MGWG must be addressed. Improved flange designs are necessary to effectively suppress leakage and resonances.

IV. CONCLUSION

This letter introduces for the first time an innovative multigap waveguide phase shifter, achieved through the segmentation of the waveguide into four distinct, dc-decoupled segments. The novel configuration utilizes the waveguide structure itself for full electrical LC biasing. A substrate is integrated for electrical breakdown coverage, and a gap waveguide flange is designed to ensure complete galvanic isolation and seamless compatibility with conventional WR28 measurement equipment. In the frequency range from 24 to 38.5 GHz, the resulting IL is ranging from 2.1 to 3.1 dB, with a maximum FoM of 105 °/dB.

REFERENCES

[1] Ericsson. (Jun. 2023). *Mobility Report*. [Online]. Available: https://www.ericsson.com/en/reports-and-papers/mobility-report/reports

[2] A. F. Molisch et al., "Hybrid beamforming for massive MIMO: A survey," *IEEE Commun. Mag.*, vol. 55, no. 9, pp. 134–141, Sep. 2017.

[3] M. Xiao et al., "Millimeter wave communications for future mobile networks," *IEEE J. Sel. Areas Commun.*, vol. 35, no. 9, pp. 1909–1935, Sep. 2017.

[4] R. Gannedahl and H. Sjöland, "An LO phase shifter with frequency tripling and phase detection in 28 nm FD-SOI CMOS for mm-wave 5G transceivers," *Anal. Integr. Circuits Signal Process.*, vol. 114, no. 1, pp. 1–11, Jan. 2023.

[5] J. Lou, Z. Zhao, Y. Ruixia, M. Lu, and X. Hu, "A DC-to-32 GHz 2-bit MEMS phase shifter," in *Proc. IEEE Antennas Propag. Soc. Symp.*, vol. 3, Jun. 2004, pp. 2867–2870.

[6] C.-H. Wu, W.-T. Li, J.-H. Tsai, and T.-W. Huang, "Design of a K-band low insertion loss variation phase shifter using 0.18-μm CMOS process," in *Proc. Asia–Pacific Microw. Conf.*, Dec. 2010, pp. 1735–1738.

[7] H. Maune, M. Jost, R. Reese, E. Polat, M. Nickel, and R. Jakoby, "Microwave liquid crystal technology," *Crystals*, vol. 8, no. 9, p. 355, Aug. 2018. [Online]. Available: https://www.mdpi.com/2073-4352/8/9/355

[8] M. Jost et al., "Tuneable hollow waveguide devices for space applications based on liquid crystal," in *IEEE MTT-S Int. Microw. Symp. Dig.*, Nov. 2015, pp. 1–5.

[9] A. Gaebler, F. Goelden, A. Manabe, M. Goebel, S. Mueller, and R. Jakoby, "Investigation of high performance transmission line phase shifters based on liquid crystal," in *Proc. Eur. Microw. Conf. (EuMC)*, Sep. 2009, pp. 594–597.

[10] R. Neuder, D. Wang, M. M. Schüßler, R. Jakoby, and A. Jiménez-Sáez, "Compact liquid crystal-based defective ground structure phase shifter for reconfigurable intelligent surfaces," in *Proc. 17th Eur. Conf. Antennas Propag. (EuCAP)*, Mar. 2023, pp. 1–5.

[11] E. Rajo-Iglesias, M. Ferrando-Rocher, and A. U. Zaman, "Gap waveguide technology for millimeter-wave antenna systems," *IEEE Commun. Mag.*, vol. 56, no. 7, pp. 14–20, Jul. 2018.

[12] M. Nickel et al., "Ridge gap waveguide based liquid crystal phase shifter," *IEEE Access*, vol. 8, pp. 77833–77842, 2020.

[13] R. Corporation. (Dec. 2023). *Rt/duroid 5870 /5880*. [Online]. Available: https://www.rogerscorp.com/advanced-electronics-solutions/rt-duroid-laminates/rt-duroid-5880-laminates

[14] E. Polat et al., "Reconfigurable millimeter-wave components based on liquid crystal technology for smart applications," *Crystals*, vol. 10, no. 5, p. 346, Apr. 2020.

[15] S. Rahiminejad, E. Pucci, V. Vassilev, P.-S. Kildal, S. Haasl, and P. Enoksson, "Polymer gap adapter for contactless, robust, and fast measurements at 220–325 GHz," *J. Microelectromech. Syst.*, vol. 25, no. 1, pp. 160–169, Feb. 2016.

[16] A. S. Daryoush, T. Sun, N. Bromhead, A. K. Poddar, and U. L. Rohde, "Computer-controlled k-band frequency synthesizer using self-injection-locked phase-locked optoelectronic oscillator: Part 2," *Microw. J.*, vol. 62, no. 9, pp. 52–66, Sep. 2019.

[17] R. Jakoby, P. Ferrari, O. H. Karabey, G. P. Rehder, and H. Maune, "5 microwave liquid crystal technology," in *Reconfigurable Circuits and Technologies for Smart Millimeter-Wave Systems*. Cambridge, U.K.: Cambridge Univ. Press, 2022, p. 265.

[18] R. De Paolis, F. Coccetti, S. Payan, M. Maglione, and G. Guegan, "Characterization of ferroelectric BST MIM capacitors up to 65 GHz for a compact phase shifter at 60 GHz," in *Proc. 44th Eur. Microw. Conf.*, Oct. 2014, pp. 492–495.

[19] D. F. Mamedes, M. Esmaeili, and J. Bornemann, "K-band substrate integrated waveguide variable phase shifter," in *Proc. 10th Eur. Conf. Antennas Propag. (EuCAP)*, Apr. 2016, pp. 1–4.